MODEL-BASED FUSION OF CT AND NON-CONTRASTED 3D C-ARM CT: APPLICATION TO TRANSCATHETER VALVE THERAPIES

Sasa Grbic[⋆†], *Christian Gesell*[⋆°], *Razvan Ionasec*[⋆], *Matthias John*[‡], *Jan Boese*[‡], *Joachim Hornegger*[°], *Nassir Navab*[†], *Dorin Comaniciu*[⋆]

[⋆] Image Analytics and Medical Informatics, Siemens Corporate Research, Princeton, USA
[†] Computer Aided Medical Procedures, Technical University Munich, Germany
[‡] Siemens AG, Healthcare Sector, Forchheim, Germany
[°] Pattern Recongnition Lab, University of Erlangen-Nuremeberg, Germany

ABSTRACT

In recent years transcatheter valve therapies are beginning to replace invasive surgical procedures. As there is no direct view and access to the affected anatomy advanced imaging techniques such as 3D rotational angiography (C-arm CT) and real-time fluoroscopy are used for intra-operative guidance. However, intra-operative modalities have limited image quality of the soft tissue and a reliable assessment of the cardiac anatomy can only be made by injecting contrast agent, which is harmful to the patient and requires complex acquisition protocols. We propose a novel method to align pre-operative and intra-operative data by using surrogate anatomical structures which are visible in both modalities without adding contrast agent. The trachea bifurcation model is used as a surrogate structure and the model parameters are estimated using robust machine learning algorithms. High quality patient specific models can be extracted from the pre-operative CT and mapped to the intra-operative 3D C-arm CT for guidance. In addition we learn a weighted mapping function for the trachea bifurcation model extracted from the pre-operative and intra-operative images which minimizes the mapping error in respect to the anatomy of interest. Experiments performed on 28 patient pairs of CT and contrasted 3D C-arm CT data sets assure an accuracy of the mapped aortic valve model of 9.08 ± 7.31deg and 7.57 ± 3.22mm.

1. INTRODUCTION

There has been a major trend in cardiac therapy towards minimally invasive procedures. Transcatheter valve interventions are becoming the standard therapy for high risk surgical patients. The procedure offers the potential to reduce procedural morbidity, mortality, and costs of surgical valve replacement or repair while accelerating patient recovery. One of the most common minimally invasive procedures is Transcatheter Aortic-Valve Implantation (TAVI) [1]. Hereby the implantation procedure involves accessing a femoral artery, performing balloon valvuloplasty, then advancing the device across the native valve. During rapid right ventricular pacing, a balloon is inflated to deploy the artificial aortic valve [2]. Having a high-quality patient-specific model from the pre-operative CT fused with the 3D C-arm CT would help the physician to position the catheter properly without having to inject contrast agent (see Fig. 1).

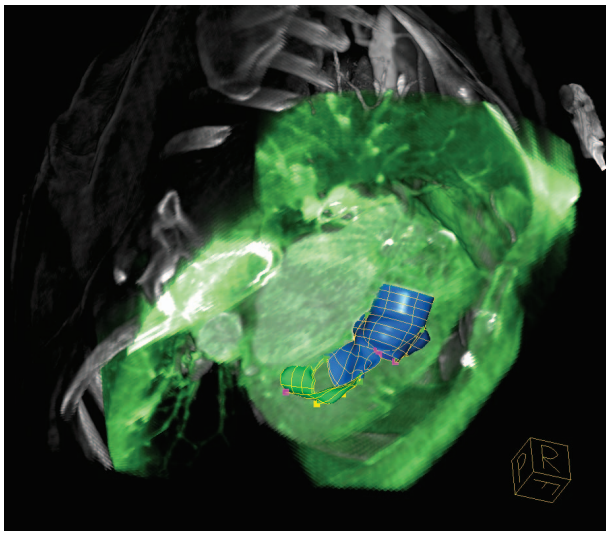


Fig. 1. Fused image (pre-operative CT and intra-operative 3D C-arm CT) with pre-operstive aortic and mitral valve models extracted from CT. The CT is shown as an grayscale image while the aligned native DynaCT is overlayed in the green color channel.

Using geometrical models for pre-operative decision making has already been proposed in current literature. The aortic valve has been segmented from 3D CT [3], while [4] estimated the aortic-mitral valve dynamic models from 4D transesophageal echocardiogram (TEE) data and [5] proposed to estimate a dynamic patient-specific model of the whole valvular apparatus from 4D CT. However these methods are designed to work on pre-operative data (CT, MRI, TEE) and are not able to cope with the limited contrast and

image quality in intra-operative modalities such as 3D C-arm CT. [6] proposed to use a joint estimation of the aortic valve model from CT and contrasted 3D C-arm CT but the method relies on contrasted 3D C-arm CT data.

Utilizing high-quality models in the operating room to guide cardiac procedures will be of major importance for upcoming clinical applications. Recent work [7] showed that intra-operative guidance can be achieved by injecting contrast agent during the acquisition of the 3D C-arm CT. Using the contrasted volume a model of the aorta could be estimated and used for TAVI guidance. [8] proposed to use TEE ultrasound to bring pre-operative models estimated from a CT image to fluoroscopy. Pre-operative models of the mitral valve annotated in pre-operative CT were fused with the intra-operative MR and echocardiography using fuduicial points on the mitral valve surface [9]. The limitation of the method is the reliance on tracking equipment and semi-automatic delineation of the mitral annulus.

We propose a novel method to fuse pre-operative and intra-operative modalities and thus map high-quality patient-specific models from the pre-operative CT to the intra-operative 3D C-arm CT without adding contrast agent. By using surrogate anatomical structures, such as the trachea bifurcation model, clearly visible in both modalities we show that a good mapping for the aortic valve can be established. The anatomy of interest, the aortic-valve, does not have to be visible in the intra-operative modality and the complex acquisition protocol of a contrasted 3D C-arm CT can be avoided. Robustness and efficiency are achieved by relying on machine learning techniques during the model estimation process. A weighted mapping function is learned from ground-truth annotations to minimize the mapping error.

2. METHOD

As we use the trachea bifurcation model as a surrogate anatomy to map the aortic valve from the pre-operative CT to the intra-operative 3D C-arm CT the modeling and automated estimation of the anatomy is a critical part of our framework.

2.1. Trachea Modeling and Estimation

The global position of the trachea bifurcation model is parameterized with a similarity transformation in the three-dimensional Cartesian space, illustrated as a bounding box in Fig. 2.

$$\Theta = \{(c_x, c_y, c_z), (\vec{\alpha}_x, \vec{\alpha}_y, \vec{\alpha}_z), (s_x, s_y, s_z)\} \qquad (1)$$

where (c_x, c_y, c_z), $(\vec{\alpha}_x, \vec{\alpha}_y, \vec{\alpha}_z)$, (s_x, s_y, s_z) are the position, orientation and scale parameters. The parameters are estimated within the marginal space famework. A probabilistic boosting tree classifier is trained based on Haar features for position and steerable features for orientation and scale, as described in [10].

The next modeling layer consists of four landmarks which are defining key anatomical properties of the trachea bifurcation model: The trachea airway bifurcation point t_B, the trachea lower-left airway branching point t_{LL}, the trachea lower-right airway branching point t_{LR} and the trachea upper center airway point t_T. Using the probabilistic boosting tree classifier and Haar features the location of each landmark is learned independently.

The full geometry of the trachea bifurcation is modeled using five surface meshes constructed along rectangular grids of vertices: The underlying grid of each surface mesh is spanned along two physiologically aligned parametric directions, $\vec{u}$ and $\vec{v}$. The trachea upper center airway model T_T, the trachea lower-left airway model T_{LL} and the trachea lower-right T_{LR} airway model are represented as a tubular grid with circumferential $\vec{u}$ and ascending $\vec{v}$ directions including 36×20 vertices. The trachea bifurcation face T_F and back T_B model are represented as paraboloids on a grid of 18×18 vertices. Every corner vertex of the face (T_F)and back model (T_B) has its corresponding vertex on the upper T_T, lower-left T_{LL} and lower-right T_{LR} surface model. The shape model is estimated using the non-rigid Marginal Space Learning framework. Hereby the search space is defined by the first three modes (c_1, c_2, c_3) computed from the statistical shape model. For each mode a boosting classifier is trained using steerable features to distinguish correct hypothesis [10].

2.2. Fusion

Our goal is to estimate the rigid transformation A consisting of a translation A_T and a rotation A_R between the pre-operative CT I_1 to the intra-operative 3D C-arm CT I_2:

$$I_1 = A\ I_2 \qquad (2)$$

Based on the detected trachea bifurcation meshes T_1 and T_2 a least squares solution is employed to estimate A_T and A_R [11]. In order to minimize the mapping error in regard to the anatomy of interest, the aortic valve, we estimate a weighting factor for each mesh point. Based on the aortic valve hinges (3 points) and the aortic valve commissures (3 points) a ground-truth mapping A_{GT} is estimated. Every intra-operative model of the trachea bifurcation T_2 is transformed to the pre-operative using: $T_{21} = A_{GT}\ T_2$ and the variance of the point-wise distance $|T_{21} - T_1|$ is computed. The weighting factor $w(i)$ for each mesh point is computed as:

$$w(i) = k\ \frac{1}{M} \sum_{j=1}^{M} |T_{21}(j,i) - T_1(j,i)| \qquad i = 1\ \ldots\ N \qquad (3)$$

where N is the number of mesh points on the trachea bifurcation surface, M the number of pair-wise mesh annotations and k a normalizing factor. The weights w are later used to

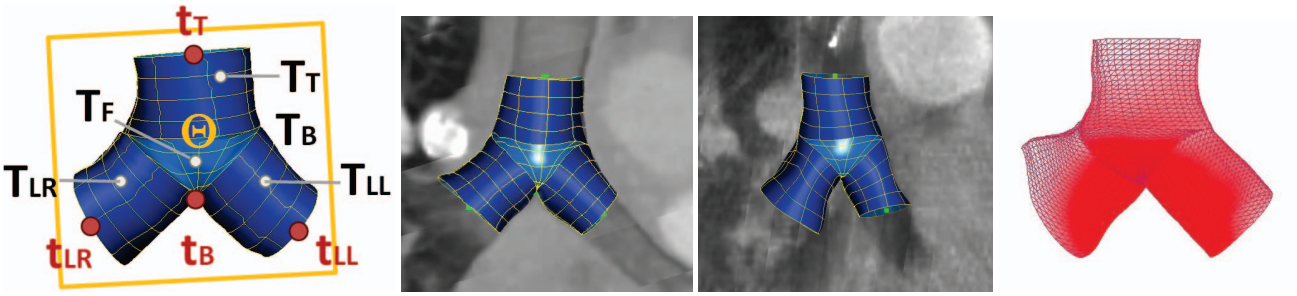


Fig. 2. The trachea bifurcation model. Left: Model showing the bounding box Θ, anatomical landmarks: trachea airway bifurcation point t_B, trachea lower-left airway branching point t_{LL}, trachea lower-right airway branching point t_{LR}, trachea upper center airway point t_T and surfaces: trachea upper center airway model T_T, trachea lower-left airway model T_{LL} and trachea lower-right T_{LR} airway model, trachea bifurcation face T_F and back T_B. Trachea bifurcation model shown in CT and 3D C-arm CT (center). The right image is showing the trachea bifurcation model with weights assigned to each vertex for pre-operative to intra-operative mapping A: white - low significance, red - high significance.

solve the weighted least squares mapping:

$$e^2(R,t) = \frac{1}{N}\sum_{i=1}^{N} \left|\left|w(i)^{-1}\ (T_2(i) - T_1(j,i))\right|\right| \quad (4)$$

The solution to this problem can be found in [11]. Fig. 2 shows the mean trachea bifurcation model with weights w assigned to each vertex.

3. EXPERIMENTAL RESULTS

In order to validate the mapping A from pre-operative CT to the intra-operative 3D C-arm CT we used 28 patient pairs (56 volumes) for our quantitative experiments. The aortic valve was annotated in the contrasted 3D C-arm CT. As we used contrasted intra-operative data the aortic valve was visible and could be delineated manually. Additional 20 test data sets, without pairs of pre-operative and intra-operative images were used to evaluate the estimation performance of the trachea bifurcation model in both the pre-operative CT and intra-operative 3D C-arm CT. All ground-truth annotations were obtained by expert users manually placing bounding boxes, anatomical landmarks in the pre- and intra-operative images and finally delineating the surface of the trachea bifurcation and the aortic valve model.

3.1. Model estimation

As our weighted mapping relies on the automatic detection of the trachea bifurcation model T we first compare the estimation results on CT and 3D C-arm CT independently. Each detector was trained based on the 28 training data and evaluated on 10 unseen volumes. The accuracy on training and test data is shown in Table 1 and 2. We compared the estimation of the bounding box Θ, the 4 bifurcation landmarks (t_B, t_{LL}, t_{LR}, t_T) and the combined mesh-to-mesh error from all 5 surfaces (T_T, T_{LL}, T_{LR}, T_F, T_B).

Table 1. System precision for the estimation of the trachea bifurcation bounding box Θ in CT and 3D C-arm CT.

	Training	
	CT	C-arm CT
Center [mm]	1.90 ± 0.69	1.98 ± 0.80
Angle [deg]	3.21 ± 1.44	3.07 ± 1.26
Scale [mm]	3.41 ± 1.70	2.73 ± 1.36
	Testing	
	CT	C-arm CT
Center [mm]	3.20 ± 1.58	3.12 ± 2.46
Angle [deg]	8.08 ± 10.26	9.26 ± 7.90
Scale [mm]	2.65 ± 0.86	3.09 ± 0.73

Table 2. System precision for the estimation of trachea bifurcation landmarks (t_B, t_{LL}, t_{LR}, t_T) and the surface ($T = T_T \cup T_{LL} \cup T_{LR} \cup T_F \cup T_B$) in CT and 3D C-arm CT.

	Training	
	CT	C-arm CT
t_B [mm]	1.96 ± 0.63	1.86 ± 0.80
t_{LL} [mm]	3.54 ± 1.47	3.62 ± 1.29
t_{LR} [mm]	3.74 ± 2.19	3.70 ± 2.06
t_T [mm]	3.22 ± 1.40	2.47 ± 1.21
T [mm]	0.82 ± 0.11	1.18 ± 0.52
	Testing	
	CT	C-arm CT
t_B [mm]	2.68 ± 1.08	3.30 ± 2.22
t_{LL} [mm]	4.70 ± 1.39	4.14 ± 2.78
t_{LR} [mm]	5.16 ± 2.95	5.52 ± 2.72
t_T [mm]	4.30 ± 1.69	4.30 ± 2.01
T [mm]	0.87 ± 0.14	1.25 ± 0.62

3.2. Model fusion

In order to validate the accuracy of our mapping from the pre-operative CT to the intra-operative 3D C-arm CT the aortic

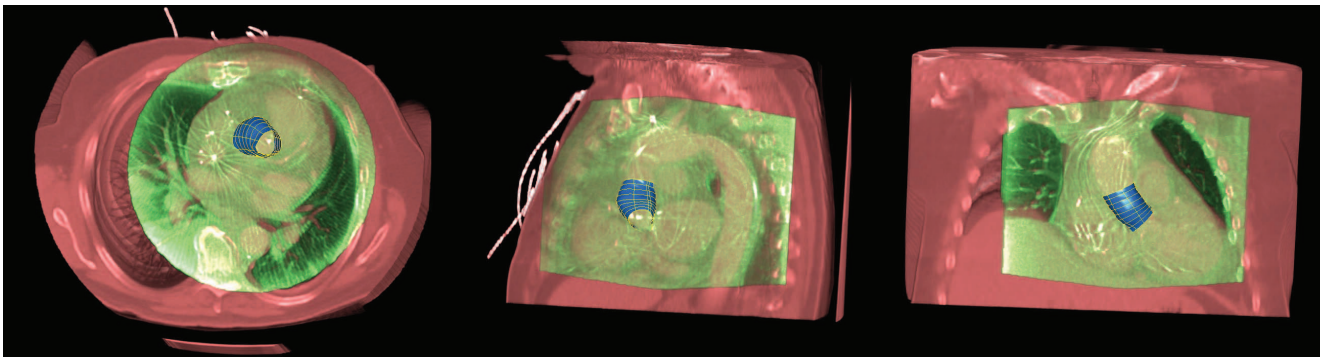


Fig. 3. Example of the aligned pre-operative CT image I_1 (red channel) with the intra-operative 3D C-arm CT I_2 (green channel) and the mapped aortic valve model.

valve was detected in CT, similar as in [5], and mapped to the intra-operative modality using our weighted mapping function A. The estimation errors could be assessed in table 3. Figure 3 shows examples of fused volumes with the mapped aortic valve model detected in pre-operative CT and mapped to the non-contrasted 3D C-arm CT.

Table 3. System precision for the estimation of aortic valve in 3D C-arm CT using the mapping estimated from the detected surrogate trachea bifurcation models T_1 and T_2 and the weighted transform A.

	Mean	STD	Median
AV Surface [mm]	7.57	3.22	8.22
Angulation [deg]	9.08	7.31	6.20

4. CONCLUSION

In this paper we presented a novel method to fuse pre-operative CT and intra-operative 3D C-arm CT data for TAVI guidance by relying on the surrogate model of the trachea bifurcation to estimate a rigid mapping between the two modalities. Complex acquisition protocols of contrasted 3D C-arm CT could be avoided as our method relies on the trachea bifurcation model which is visible in both modalities without adding contrast. A weighted mapping transform is learned from training data to minimize the estimation error of the anatomy of interest, the aortic valve. Fast and robust machine learning algorithms are employed to estimate the final model parameters which can handle noisy intra-operative data. Comprehensive qualitative and quantitative experiments demonstrate an efficient estimation of the trachea bifurcation model and a precise mapping of detected aortic valve model from pre-operative CT to the non-contrasted 3D C-arm CT within ten seconds and an accuracy of 9.08 ± 7.31deg and 7.57 ± 3.22mm. Thus comprehensive, patient-specific models can be estimated from high-contrast CT and fused into the imaging environment of operating rooms to guide cardiac interventions. Further work will focus on improving the mapping accuracy and investigating other anchor anatomies besides the trachea bifurcation model to calculate the transformation between the pre-operative CT and the intra-operative 3D C-arm CT.

5. REFERENCES

[1] S. Ewe et al., "Role of computed tomography imaging for transcatheter valvular repair/insertion," *Journal of Cardiovascular Imaging*, 2011.

[2] C. Schultz et al., "Cardiac ct: necessary for precise sizing for transcatheter aortic implantation," *Eurointervention*, pp. 6–13.

[3] I. Waechter et al., "Patient specific models for planning and guidance of minimally invasive aortic valve implantation," in *MICCAI*, 2010, pp. 526–533.

[4] R. Ionasec et al., "Patient-specific modeling and quantification of the aortic and mitral valves from 4-D cardiac CT and TEE.," *TMI*, vol. 29, no. 9, pp. 1636–51, 2010.

[5] S. Grbic et al., "Complete valvular heart apparatus model from 4D cardiac CT.," in *MICCAI*, 2010, vol. 13, pp. 218–26.

[6] S. Grbic et al., "Model-based fusion of multi-modal volumetric images: application to transcatheter valve procedures," in *MICCAI*, 2011, pp. 219–226.

[7] Y. Zheng et al., "Automatic aorta segmentation and valve landmark detection in c-arm ct: application to aortic valve implantation.," in *MICCAI*, 2010, vol. 13, pp. 476–483.

[8] P. Lang et al., "Feature-based US to CT registration of the aortic root," in *Proceedings of SPIE Medical Imaging 2010*, 2010.

[9] C. Linte et al., "Towards subject-specific models of the dynamic heart for image-guided mitral valve surgery," in *MICCAI*, 2007, pp. 94–101.

[10] Y. Zheng et al., "Marginal space learning for efficient detection of 2d/3d anatomical structures in medical images.," in *IPMI*, 2009, vol. 5636, pp. 411–422.

[11] S. Umeyama, "Least-squares estimation of transformation parameters between two point patterns," *PAMI*, vol. 13, no. 4, pp. 376 –380, apr 1991.